Intercomparison of Deep Convective Cloud Fractions from Passive Infrared and Microwave Radiance Measurements

Gang Hong, Georg Heygster, *Member, IEEE*, and Klaus Kunzi, *Senior Member, IEEE*

***Abstract*— The common method to detect deep convective clouds is from satellite infrared measurements, which is based on thresholds of cloud top temperatures. However, thick cirrus clouds with high cloud top are difficult to screen out using IR methods resulting in an overestimation of deep convective cloud fractions. Two aircraft cases with simultaneous Millimeter-wave Imaging Radiometer (MIR), Multispectral Atmospheric Mapping Sensor (MAMS), and ER-2 Doppler radar (EDOP) measurements during the Convection And Moisture EXperiment (CAMEX)-3 in August 1998 are analyzed to investigate the influence of high thick cirrus clouds on two previously developed IR methods. In contrast, a microwave method based on the brightness temperature differences between the three water vapor channels around 183.3 GHz of the Advanced Microwave Sounder Unit (AMSU)-B (183.3 ± 1, 183.3 ± 3, and 183.3 ± 7 GHz) can screen out high thick cirrus clouds efficiently. The tropical deep convective cloud fractions (30° S–30° N) estimated by the IR methods and the AMSU-B method are compared. Although their geographical distributions are in well agreement with each other, the total fractions detected by the IR methods are about 2 to 3.5 times greater than that detected by the AMSU-B method. Moreover, the overestimation of deep convective cloud fractions by the IR method (11 μm brightness temperature less than 215 K) can result in a displacement in the detected location of the deep convective clouds. The average thick cirrus clouds cover 2.5 times the area of the deep convective clouds that generates them.**

***Index Terms*— Deep convective cloud, infrared radiance, microwave radiance, AMSU-B.**

I. Introduction

Deep convective cloud is a more vertically developed and localized convective event that is characterized by rapid injection of boundary layer air near or through the tropopause (e.g., [1]). It plays a major role in the Earth's climate by transporting heat, moisture, and momentum from the lower to the upper troposphere. Convective clouds penetrating into the tropical tropopause layer (TTL, about 14–18 km above the surface) contribute to the exchange of air between the troposphere and the stratosphere, and hereby influence the physical and chemical processes occurring in the TTL and the stratosphere (e.g., [2]–[7]).

Knowing quantitatively the frequencies, heights, and locations of deep convective clouds accurately is not only important for climate modeling (e.g., [1], [8], [9]), but also a critical prerequisite for understanding their influence on the physical and chemical processes occurring in the TTL and the stratosphere (e.g., [10] and [11]). In addition to ground-based cloud observations, satellite data including passive measurements of visible, infrared, and microwave radiances and active radar measurements have been used in the studies of deep convective clouds (e.g., [1], [4], [9], [10], [12]).

Since geostationary satellites provide frequent observations with wide spatial coverage, the most common method to identify tropical deep convective clouds is from such infrared (IR) measurements. It is based on thresholds of cloud top temperatures. Different thresholds of IR brightness temperature at 11 μm wavelength have been used, e.g., 208 K by Hall and Haar [9], 215 K by Fu et al. [13] and Gettelman et al. [4], 230 K by Hendon and Woodberry [14] and Tian et al. [15], and 233 K by Liu et al. [12]. Cirrostratus and cirrocumulus clouds are mainly generated from deep convective clouds [16]. Fu et al. [13] suggested a sufficiently cold IR threshold at 215 K to distinguish deep convective clouds from their associated anvil cirrus. Inoue [17], [18] used brightness temperature differences between the split window channels (11 and 12 μm) to classify optically thick cloud and optically thin cloud. However, the methods based on IR radiance have the disadvantage to infer the properties of deep convective clouds because IR sensors do not sense directly radiation from their interior [12], [19].

Passive microwave sensors measure the effects of scattering of upwelling radiation due to precipitation size ice particles in the upper layers of convective systems at frequencies above 150 GHz (e.g., [20]–[23]). A passive microwave method based on the brightness temperature differences between the three water vapor channels around 183.3 GHz of the Advanced Microwave Sounder Unit (AMSU)-B was developed by Hong et al. [24]. The detected tropical deep convective cloud fractions by their method are much lower than those detected by IR methods. This was explained by the exclusion of thick cirrus cloud fractions from deep convective cloud fractions by this method. Also radar observations can be used to detect deep convective clouds. However, passive microwave observations provide the advantage of a much higher global coverage, repeat cycle and total observation period. E.g. with the three sensors AMSU-B aboard the NOAA-15, 16 and 17 satellites currently in orbit, each point on earth is observed six times per day, and together with the similar Special Sensor Microwave Water Vapor Profiler (SSM/T2) sensors aboard the Defense Meteorological Satellite Program (DMSP) satellites, continuous observations since 1992 are available.

G. Hong, G. Heygster, and K. Kunzi are with the Institute of Environmental Physics, University of Bremen, Post Box 330440, Bremen 28203, Germany. (honggang@uni-bremen.de)

The purpose of this study is to investigate the influence of thick cirrus clouds on the estimation of deep convective cloud fractions. Here we compare deep convective cloud fractions detected from IR radiances against those from microwave radiances. Two aircraft cases obtained during the Convection And Moisture EXperiment (CAMEX)-3 are analyzed with simultaneous IR radiances, microwave radiances, and radar observations. One month of AMSU-B and the High Resolution Infrared Radiation Sounder (HIRS) data onboard NOAA-16 in July 2001 are employed to compare the estimation of tropical deep convective clouds (30° S–30° N).

II. Aircraft Observations

The NASA ER-2 aircraft flying at an altitude of about 20 km was equipped with microwave, visible and IR radiometers, and radar instruments during the campaign CAMEX-3 based at Patrick Air Force Base, Florida from 6 August to 23 September, 1998. Two cases observed along the ER-2 straight flight tracks from 21:17:17 to 21:39:16 UTC (from (71.02° W, 25.29° N) to (73.02° W, 23.44° N)) on 23 August 1998 and from 16:04:49 to 16:12:20 UTC (from (79.46° W, 34.16° N) to (79.84° W, 33.38° N)) on 26 August 1998 over ocean are used in this study. Both of them include simultaneous observations by the Millimeter-wave Imaging Radiometer (MIR), the Multispectral Atmospheric Mapping Sensor (MAMS), and the ER-2 Doppler radar (EDOP) [25]. The MIR observed at frequencies from 89 to 340 GHz. The three water vapor channels around 183.3 GHz (183.3 ± 1, 183.3 ± 3, 183.3 ± 7 GHz), the same as those of AMSU-B, are employed to detect deep convective clouds using the method of Hong et al. [24] (hereafter referred to as the AMSU-B method). The MAMS measured reflected radiation from the surface and clouds in eight visible/near IR bands (0.4–1.0 μm), and thermal emission from water vapor, the surface and clouds, in four IR bands (6.0–13 μm). The MAMS data of interest in this study are 11.12 and 12.56 μm IR data, which detect deep convective clouds using the threshold method of Fu et al. [13] and the split window method of Inoue [18]. The EDOP radar samples at 9.6 GHz with a vertical resolution of 37.5 m. It can provide direct information on vertical cloud structure. The EDOP radar and MIR measurements at nadir and the MAMS averaged measurements from the two viewing angles closest to nadir are used in this study.

Fig. 1 shows the collocated observations in the flight track from 21:17:17 to 21:39:16 UTC on 23 August 1998, including the MAMS observed brightness temperatures at 11 μm (T_{11}) and brightness temperature difference between 11 and 12 μm ($\Delta T_{\rm IR} = T_{11} - T_{12}$), the observed brightness temperature differences between 183.3 ± 1 and 183.3 ± 7 (ΔT_{17}) , 183.3 ± 1 and 183.3 ± 3 (ΔT_{13}) , and 183.3 ± 3 and 183.3 ± 7 GHz (ΔT_{37}) from the MIR, and the EDOP radar reflectivities. The EDOP radar reflectivities (Fig. 1(c)) show that clouds along this flight track include shallow convective (from 21:17:00 to 21:20:00 UTC and from 21:37:00 to 21:39:00 UTC), deep convective (from 21:21:30 to 21:24:00 UTC), and cirrocumulus (from 21:25:00 to 21:35:00 UTC) clouds.

The method of Fu et al. [13] (deep convective clouds are present when $T_{11} < 215$ K, black dotted line in Fig. 1(a), hereafter referred to as IR method 1) can discriminate deep convective clouds from shallow convective clouds, but cirrocumulus clouds are also detected as deep convective clouds. This method results in a large overestimation of deep convective cloud fractions. Even if we use a lower threshold at 208 K suggested by Hall and Haar [9], most parts of the cirrocumulus clouds still cannot be discriminated. Using lower thresholds misses the deep convective clouds with cloud top below the height corresponding to this threshold temperature, e.g., using a threshold at 208 K will result in the non-detection of deep convective clouds with cloud top height below 15 km. If applying the additional condition that deep convective clouds are present only when $\Delta T_{\rm IR} < 1$ K [18] (blue dotted line in Fig. 1(a), hereafter referred to as IR method 2), the overestimation of the occurrence of deep convective clouds caused by cirrocumulus clouds still remains but decreases with respect to the IR method 1. The AMSU-B method (deep convective clouds are present when $\Delta T_{17} \geq T_{\rm D}$, $\Delta T_{13} \geq T_{\rm D}$, and $\Delta T_{37} \geq T_{\rm D}$, with the threshold being a function of the AMSU-B viewing angle θ with $T_{\rm D} = 0.05 - 0.02\,\theta + 0.006\,\theta^2$, Fig. 1(b)) detects the deep convective clouds extremely well.

Fig. 2 shows the collocated observations from the same instruments as in Fig. 1 along the flight track from 16:04:49 to 16:12:20 UTC on 26 August 1998. The EDOP radar reflectivities (Fig. 2(c)) show that cirrostratus clouds with tops around 14 km were found along the entire flight track. All T_{11} values are below 215 K and most of them are below 208 K. The IR method 1 estimates all cirrostratus clouds as deep convective clouds. $\Delta T_{\rm IR}$ is noisy, but generally constant around 3 K. Thus, it is well above the threshold value of 1 K. The cirrostratus clouds in this case are screened out by the IR method 2. There are no cloud regions with $\Delta T_{17} \geq 0$, $\Delta T_{13} \geq 0$, and $\Delta T_{37} \geq 0$ K (Fig. 2(b)). This confirms that the estimation of the deep convective cloud fraction from the AMSU-B method is not influenced by cirrostratus clouds.

We conclude from Figs. 1 and 2 that there exists no appropriate threshold values neither for the IR threshold of the IR method 1 nor for the additional threshold $\Delta T_{\rm IR}$ of the IR method 2 that allows to separate deep convective clouds against high thick cirrus clouds. However, the AMSU-B method clearly can distinguish high thick cirrus clouds. Therefore, we will use the AMSU-B method as a reference when applying all three methods to satellite data in the next section.

III. Satellite Observations

Data of the NOAA-16 HIRS IR 11.11 and 12.47 μm channels and of the AMSU-B water vapor channels (183.3 ± 1, 183.3 ± 3, and $183,3 \pm 7$ GHz) collected in July 2001 are used to estimate the distributions of tropical deep convective clouds by the three methods discussed above. Deep convective clouds are averaged over $1^\circ \times 1^\circ$ longitude-latitude grid boxes in the topics (30° S–30° N). Fig. 3 shows the distributions of deep convective clouds as resulting from the three methods and the overestimation of deep convective cloud fractions by the IR method 1 with respect to those detected by the AMSU-B method.

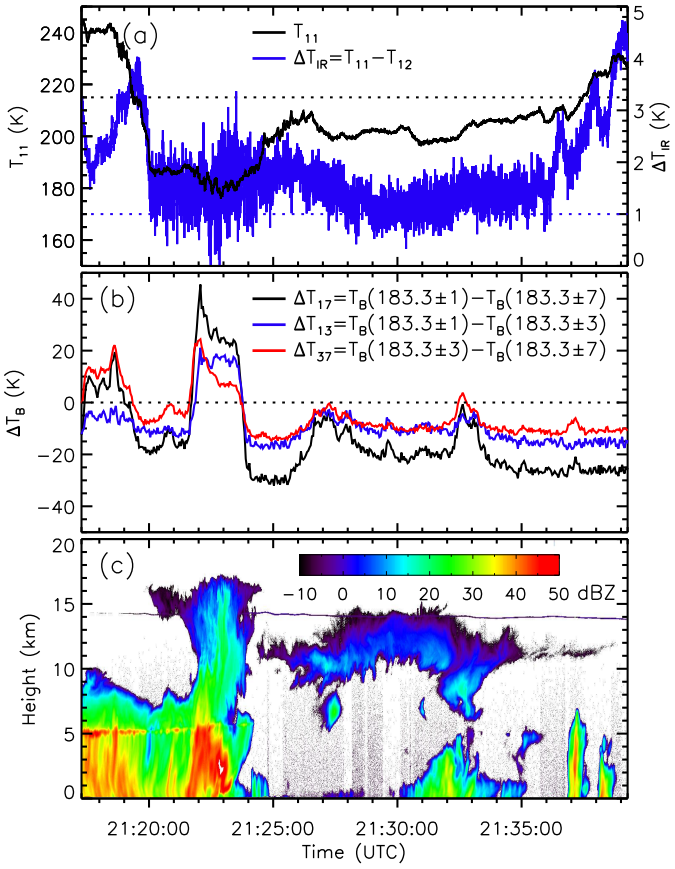

Fig. 1. Time series of radiometric and radar data along the flight track from 21:17:17 to 21:39:16 UTC on 23 August 1998 during CAMEX-3 (1 min ≈ 13 km). (a) IR brightness temperature at 11 μm and IR brightness temperature difference between 11 and 12 μm observed from MAMS, the black dotted line ($T_{11} = 215$ K) is the threshold of the IR method 1, the blue dotted line ($\Delta T_{\rm IR} = 1$ K) is the additional threshold of the IR method 2, $\Delta T_{\rm IR}$ is smoothed with a window of 0.5 s. For (b) and (c) see Fig. 2.

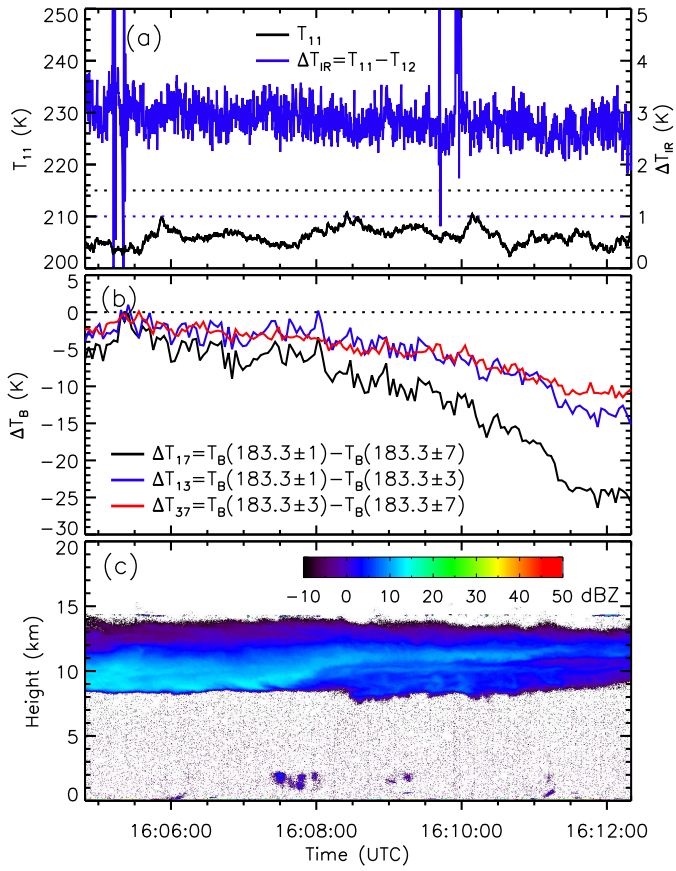

Fig. 2. Same as Fig. 1 but for the flight track from 16:04:49 to 16:12:20 UTC on 26 August 1998 over a cirrostratus cloud. (a) see Fig. 1, (b) microwave brightness temperature differences between the three water vapor channels around 183.3 GHz observed from MIR, the black dotted line ($\Delta T_{\rm D} = 0$ K) is the threshold of the AMSU-B method at nadir, (c) EDOP reflectivity cross sections.

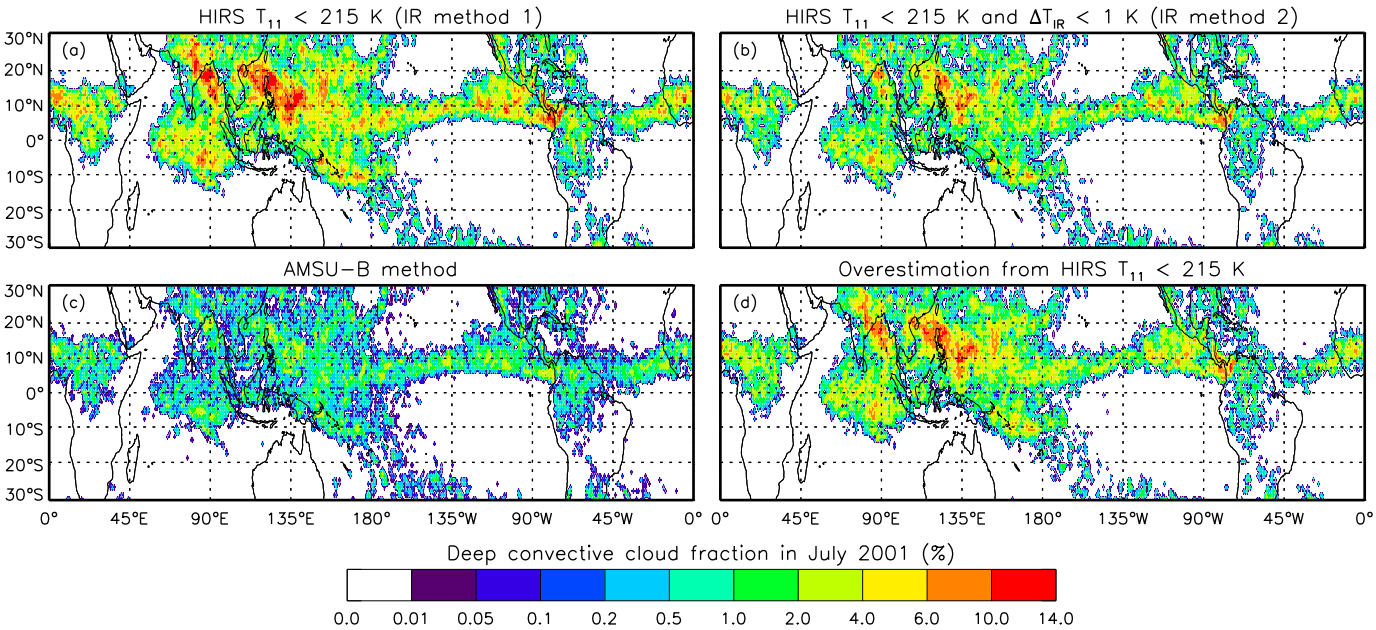

Fig. 3. The distributions of deep convective cloud fractions in the tropics detected from HIRS and AMSU-B in July 2001, (a) HIRS $T_{11} < 215$ K (the IR method 1), (b) HIRS $T_{11} < 215$ K and $\Delta T_{\rm IR} < 1$ K (the IR method 2), (c) the AMSU-B method, (d) overestimation of deep convective cloud fractions detected by the IR method 1 with respect to those detected by the AMSU-B method.

The geographical distributions of deep convective clouds detected by the three methods are in well agreement with each other (Fig. 3(a)–(c)). Their similar characteristics include the pronounced Intertropical Convergence Zone (ITCZ) across the Pacific and the Atlantic Oceans, the pronounced South Pacific Convergence Zone (SPCZ), intense centers of convection over tropical Africa, tropical America, the Indian Ocean, and southeast Asia. These intense centers over southeast Asia are the strongest with respect to other regions of deep convective clouds detected by the two IR methods. However, this behavior is not confirmed by the AMSU-B method.

Obviously the IR method 1 overestimates deep convective cloud fractions because of the influence of high cirrus clouds (Fig. 3(a)). Although the additional threshold of $\Delta T_{\rm IR} < 1$ K [18] can screen out some of them (Fig. 3(b)), overestimation is still apparent. The total fractions in Fig. 3(a) and (b) are about 3.5 and 2.2 times greater than that in Fig. 3(c). The overestimation of deep convective cloud fractions detected by the IR method 1 with respect to those detected by the AMSU-B method are very large (Fig. 3(d)). The regions with the higher deep convective cloud fractions have higher overestimation. In contrast to the airborne examples of Figs. 1 and 2, the additional threshold does not help sufficiently to screen out the high thick cirrus cloud cases. In total, it reduces the overestimation only by about 40%. There are also few underestimation cases because the threshold of $T_{11} < 215$ K misses detecting the deep convective clouds with cloud top below about 13 km, which can be detected by the AMSU-B method. If we consider the result of the IR method 1 in Fig. 3(a) as a preliminary measure of the union of the fractions of deep convective clouds and high thick cirrus clouds, then the difference (Fig. 3(d)) between the IR method 1 and the AMSU-B method would represent the thick cirrus cloud fraction alone. With this interpretation, we can confirm from Figs. 3(a) and (d) the finding of (e.g., [16], [26]) that thick cirrus clouds are generated from deep convective clouds. Moreover, we can state quantitatively that on the average thick cirrus clouds cover 2.5 times the area of the deep convective clouds that generates them, underlining the important role of the deep convective clouds for the radiation balance. The total overestimation by the IR methods 1 and 2 in the tropics in July 2001 (Fig. 3) is about 45 and 11 times greater than the total underestimation respectively, so overestimation is by far the dominant difference between the IR methods and the AMSU-B method.

Fig. 4 shows the monthly zonal means of deep convective cloud fractions detected by the IR methods and the AMSU-B method and surface rainfall from the Tropical Rainfall Measuring Mission (TRMM) 3B43 product for July 2001 [27]. All deep convective cloud fractions display similar distributions, although they have differences in magnitude. The average values of fractions detected by the IR methods 1 and 2 and the AMSU-B methods are 1.05%, 0.65%, and 0.30%, respectively. Also the surface rainfall shows a similar shape. The correlations between surface rainfall and fractions detected by the IR methods 1 and 2, and AMSU-B method are 0.94, 0.96, and 0.98, respectively. The latitude of the peak of fractions detected by the AMSU-B method matches that of the surface rainfall very well (8° N). However, the peak of fractions detected by the IR method 1 lags about two degrees to the North. This reveals that deep convective clouds dominantly generate at low northern latitudes near the equator with an maximum of 8° N and they generate cirrus clouds which then are transported to higher latitude in northern summer. The overestimation of deep convective cloud fractions caused by outflowing cirrus clouds detected by the IR method 1 can result in a displacement in the detected location of the deep convective clouds.

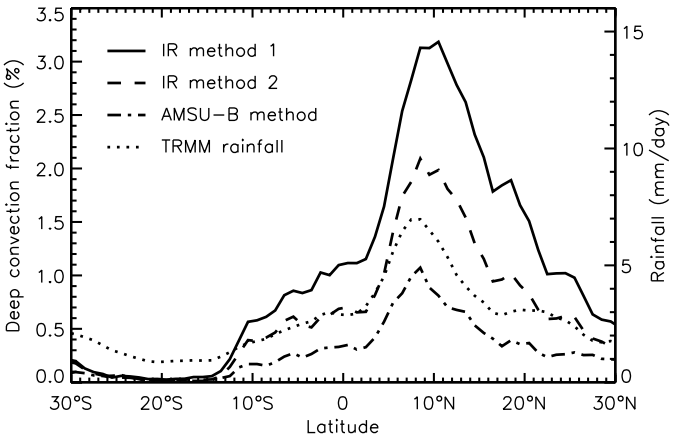

Fig. 4. Monthly zonal means of deep convective cloud fractions detected from AMSU-B and HIRS and the surface rainfall derived from the TRMM 3B43 rainfall product in July 2001.

IV. Conclusion

Two aircraft cases observed by the simultaneous MAMS, MIR, and EDOP radar instruments during CAMEX-3 were investigated to explain the overestimation of deep convective cloud fractions when using the IR methods with temperature thresholds because of the influence of thick cirrus clouds (Figs. 1 and 2). The AMSU-B method of Hong et al. [24] efficiently screens out high thick cirrus clouds. The tropical deep convective cloud fractions (30° S–30° N) are estimated by the IR methods and the AMSU-B method (Fig. 3). The geographical distributions of deep convective clouds detected by the different methods are in well agreement with each other. However, the total fractions estimated by the IR methods are about 2 to 3.5 times greater than those estimated by the AMSU-B method. Moreover, the overestimation of deep convective cloud fractions detected by the IR method ($T_{11} <$ 215 K) can result in a displacement in the detected location of the deep convective clouds. With an additional threshold ($\Delta T_{\rm IR} < 1$ K) [18], the influence of high thick cirrus clouds on IR methods is still large although some of them can be screened out. We also found that the high thick cirrus clouds are generated from deep convective clouds. The average thick cirrus clouds cover 2.5 times the area of the deep convective clouds that generates them.

The most common method to study deep convective cloud climatology is using the method of IR threshold (e.g., [4], [8], [9], [14], [15], [29]). The overestimation of deep convective cloud fractions detected by the IR methods probably results

in somewhat different characteristics of deep convective cloud climatology. First, the spatial distribution of deep convective clouds can be shifted because of outflowing cirrus clouds. Second, cirrus clouds generated by deep convective clouds can expand greatly in area and persist for some hours in the absence of deep convective clouds (e.g., [30] and [31]), so that the time of appearance of the maximum deep convective cloud fraction detected by IR methods probably lags some hours with respect to the real one. This is also questioned by Slingo et al. [32] comparing the diurnal cycle of deep convective clouds in a climate model and from satellite IR data. The AMSU-B and similar AMSU/HSB (Humidity Sounder for Brazil) sensors onboard the platforms NOAA-15, 16, 17, and Aqua can observe each point on earth about eight times per day [28]. These platforms carry also IR sensors. So combining measurements of AMSU-B and IR sensors can contribute an improved understanding of deep convective cloud climatology.

ACKNOWLEDGMENT

We wish to thank J. Wang and P. Racette for production of the MIR data; G. Heymsfield and N. Ferreira for the production of the EDOP data; R. Wohlman for providing the MAMS data; O. Lemke, M. Kuvatov, and V. John for helping us reading the AMSU-B and HIRS data. We also thank the Distributed Active Archive Center (DAAC) at the Goddard Space Flight Center, which archives and distributes the EDOP, MAMS, and MIR data under sponsorship of NASA's Earth Science Enterprise. The AMSU-B and HIRS data provided by L. Neclos from the Comprehensive Large Array-data Stewardship System (CLASS) of NOAA are taken from the Satellite Microwave Atmospheric Sounding Group at University of Bremen. The rainfall data used in this study were acquired as part of the TRMM. G. Hong is grateful to the Gottlieb Daimler- und Karl Benz- Foundation and University of Bremen for their support.

REFERENCES

[1] J. H. Jiang, B. Wang, K. Goya, K. Hocke, S. D. Eckermann, J. Ma, D. L. Wu, and W. J. Read, "Geographical distribution and interseasonal variability of tropical deep convection: UARS MLS observations and analyses", *J. Geophys. Res.*, vol. 109, D03111, doi:10.1029/2003JD003756, 2004.

[2] J. Lelieveld, and P. J. Crutzen, "Role of deep convection in the ozone budget of the troposphere", *Science*, vol. 264, pp. 1759–1761, 1994.

[3] J. R. Holton, P. H. Haynes, A. R. Douglass, R. B. Rood, and L. Pfister, "Stratosphere-troposphere exchange", *Rev. Geophys.*, vol. 33, pp. 403–439, 1995.

[4] A. Gettelman, M. L. Salby, and F. Sassi, "The distribution and influence of convection in the tropical tropopause region", *J. Geophys. Res.*, vol. 107, 4080, doi:10.1029/2001JD001048, 2002.

[5] C. Andronache, L. J. Donner, C. J. Seman, and R. S. Hemler, "A study of the impact of the Intertropical Convergence Zone on aerosols during INDOEX", *J. Geophys. Res.*, vol. 107, 8027, doi:10.1029/2001JD900248, 2002.

[6] A. E. Dessler, "The effect of deep, tropical convection on the tropical tropopause layer", *J. Geophys. Res.*, vol. 107, 4033, doi:10.1029/2001JD000511, 2002.

[7] J. Notholt, Z. Kuang, C. P. Rinsland, G. C. Toon, M. Rex, N. J. T. Albrecht, H. Deckelmann, J. Krieg, C. Weinzierl, H. Bingemer, R. Weller, and O. Schrems, "Enhanced upper tropical tropospheric COS: Impact on the stratospheric aerosol layer", *Science*, vol. 300, pp. 307–310, 2003.

[8] S. S. Chen, R. A. Houze Jr., and B. E. Mapes, "Multiscale variability of deep convection in relationship to large-scale circulation in TOGA COARE", *J. Atmos. Sci.*, vol. 53, pp. 1380–1409, 1996.

[9] T. J. Hall, and T. H. V. Haar, "The diurnal cycle of west Pacific deep convection and its relation to the spatial and temporal variations of tropical MCSs", *J. Atmos. Sci.*, vol. 56, pp. 3401–3415, 1999.

[10] C. M. Alcala, and A. E. Dessler, "Observations of deep convection in the tropics using the Tropical Rainfall Measuring Mission (TRMM) precipitation radar", *J. Geophys. Res.*, vol. 107, 4792, doi:10.1029/2002JD002457, 2002.

[11] S. C. Sherwood, H.-H. Chae, P. Minnis, and M. McGill, "Underestimation of deep convective cloud tops by thermal imagery", *Geophys. Res. Lett.*, vol. 31, L11102, doi:10.1029/2004GL019699, 2004.

[12] G. Liu, J. A. Curry, and R.-S. Sheu, "Classification of clouds over the western equatorial Pacific Ocean using combined infrared and microwave satellite data", *J. Geophys. Res.*, vol. 100, pp. 13,811–13,826, 1995.

[13] R. Fu, A. D. D. Genio, and W. B. Rossow, "Behavior of deep convective clouds in the tropical Pacific deduced from ISCCP radiances", *J. Climate*, vol. 3, pp. 1129–1152, 1990.

[14] H. H. Hendon, and K. Woodberry, "The diurnal cycle of tropical convection", *J. Geophys. Res.*, vol. 98, pp. 16,623–16,637, 1993.

[15] B. Tian, B. J. Soden, and X. Wu, "Diurnal cycle of convection, clouds, and water vapor in the tropical upper troposphere: Satellites versus a general circulation model", *J. Geophys. Res.*, vol. 109, D10101, doi:10.1029/2003JD004117, 2004.

[16] C. Chou, and J. D. Neelin, "Cirrus detrainment-temperature feedback", *Geophys. Res. Lett.*, vol. 26, pp. 1295–1298, 1999.

[17] T. Inoue, "A cloud type classification with NOAA 7 split-window measurements", *J. Geophys. Res.*, vol. 92, pp. 3991–4000, 1987.

[18] T. Inoue, "Deep convection observed from split windows of GOES and PR/TRMM, LIS/TRMM", paper presented at 84th American Meteorological Society (AMS) Annual Meeting, Amer. Meteor. Soc., Seattle, WA, 2003.

[19] C.-H. Sui, Y. N. Takayabu, and D. A. Short, "Diurnal variation in tropical oceanic cumulus convection during TOGA COARE", *J. Atmos. Sci.*, vol. 54, pp. 639–655, 1997.

[20] J. R. Wang, J. Zhan, and P. Racette, "Storm-associated microwave radiometric signatures in the frequency range of 90–220 GHz", *J. Atmos. Ocean Technol.*, vol. 14, pp. 13–31, 1997.

[21] B. A. Burns, X. Wu, and G. R. Diak, "Effects of precipitation and cloud ice on brightness temperatures in AMSU moisture channels", *IEEE Trans. Geosci. Remote Sens.*, vol. 35, pp. 1429–1437, 1997.

[22] G. M. Skofronick-Jackson, A. J. Gasiewski, and J. R. Wang, "Influence of microphysical cloud parameterizations on microwave brightness temperatures", *IEEE Trans. Geosci. Remote Sens.*, vol. 40, pp. 187–196, 2002.

[23] R. Bennartz, and P. Bauer, "Sensitivity of microwave radiances at 85–183 GHz to precipitating ice particles", *Radio Sci.*, vol. 38, 8075, doi:10.1029/2002RS002626, 2003.

[24] G. Hong, G. Heygster, J. Miao, and K. Kunzi, "Detection of tropical deep convective clouds from AMSU-B water vapor channels measurements", *submitted to J. Geophys. Res.*, Apr. 2004.

[25] G. M. Heymsfield, J. M. Shepherd, S. W. Bidwell, W. C. Boncyk, I. J. Caylor, S. Ameen, and W. S. Olson, "Structure of Florida thunderstorms using high-altitude aircraft radiometer and radar observations", *J. Appl. Meteorol.*, vol. 35, pp. 1736–1762, 1996.

[26] J. M. Comstock, and C. Jakob, "Evaluation of tropical cirrus cloud properties derived from ECMWF model output and ground based measurements over Nauru Island", *Geophys. Res. Lett.*, vol. 31, L10106, doi:10.1029/2004GL019539, 2004.

[27] G. J. Huffman, R. F. Adler, P. Arkin, A. Chang, R. Ferraro, A. Gruber, J. Janowiak, A. McNab, B. Rudolf, and U. Schneider, "The Global Precipitation Climatology Project (GPCP) combined precipitation dataset", *Bull. Amer. Meteor. Soc.*, vol. 78, 5–20, 1997.

[28] F. W. Chen, and D. H. Staelin, "AIRS/AMSU/HSB precipitation estimates", *IEEE Trans. Geosci. Remote Sens.*, vol. 41, 410–417, 2003.

[29] L. A. T. Machado, H. Laurent, and A. A. Lima, "Diurnal march of the convection observed during TRMM-WETAMC/LBA", *J. Geophys. Res.*, vol. 107, 8064, doi:10.1029/2001JD000338, 2002.

[30] H. K. Weickmann, A. B. Long, and L. R. Hoxit, "Some examples of rapidly growing oceanic cumulonimbus clouds", *Mon. Wea. Rev.*, vol. 105, pp. 469–476, 1977.

[31] W. M. Gray and R. W. Jacobson Jr., "Diurnal variation of deep cumulus convection", *Mon. Wea. Rev.*, vol. 105, pp. 1171–1188, 1977.

[32] A. Slingo, K. I. Hodges, and G. J. Robinson, "Simulation of the diurnal cycle in a climate model and its evaluation using data from Meteosat 7", *Q. J. R. Meteorol. Soc.*, vol. 130, pp. 1449–1467, 2004.